Journal of Anatomy

J. Anat. (2015) **226**, pp420–433 doi: 10.1111/joa.12291

Diversity in primary palate ontogeny of amniotes revealed with 3D imaging

John Abramyan, Beatrice Thivichon-Prince and Joy Marion Richman

Faculty of Dentistry, Life Sciences Institute, University of British Columbia, Vancouver, BC, Canada

Abstract

The amniote primary palate encompasses the upper lip and the nasal cavities. During embryonic development, the primary palate forms from the fusion of the maxillary, medial nasal and lateral nasal prominences. In mammals, as the primary palate fuses, the nasal and oral cavities become completely separated. Subsequently, the tissue demarcating the future internal nares (choanae) thins and becomes the bucconasal membrane, which eventually ruptures and allows for the essential connection of the oral and nasal cavities to form. In reptiles (including birds), the other major amniote group, primary palate ontogeny is poorly studied with respect to prominence fusion, especially the formation of a bucconasal membrane. Using 3D optical projection tomography, we found that the prominences that initiate primary palate formation are similar between mammals and crocodilians but distinct from turtles and lizards, which are in turn similar to each other. Chickens are distinct from all non-avian lineages and instead resemble human embryos in this aspect. The majority of reptiles maintain a communication between the oral and nasal cavities via the choanae during primary palate formation. However, crocodiles appear to have a transient separation between the oral and nasal cavities. Furthermore, the three lizard species examined here, exhibit temporary closure of their external nares via fusion of the lateral nasal prominences with the frontonasal mass, subsequently reopening them just before hatching. The mechanism of the persistent choanal opening was examined in chicken embryos. The mesenchyme posterior/dorsal to the choana had a significant decline in proliferation index, whereas the mesenchyme of the facial processes remained high. This differential proliferation allows the choana to form a channel between the oral and nasal cavities as the facial prominences grow and fuse around it. Our data show that primary palate ontogeny has been modified extensively to support the array of morphological diversity that has evolved among amniotes.

Key words: amniote; bucconasal membrane; choana; choanal atresia; craniofacial; nasal cavity; primary palate.

Introduction

Living amniotes can be divided into two main lineages, mammals and reptiles (including birds). Since their divergence ~ 300 million years ago, amniotes have diversified into a vast assortment of shapes and sizes with diverse life history trajectories (Benton, 1990). Although the diversity generated during evolution can be observed in general body shape and sheer size differences, a considerable amount of this diversity is concentrated in the craniofacial region. This phenomenon is in part due to specialized sensory organs and adaptations for feeding which are found in the head (Manzanares & Nieto, 2003). The diversity in adult morphology is likely initiated during embryonic development, although these interspecific differences may be subtle at early stages of facial development (Abzhanov et al. 2004; Young et al. 2014).

Facial development involves complex morphological processes that occur shortly after neurulation. Hox-negative neural crest cells migrating ventrally from the fore, mid- and hindbrain, form the majority of mesenchyme in the face (Le Douarin et al. 2007). The skeletal patterning (Richman & Lee, 2003) as well as the species-specific size of the jaws (Eames & Schneider, 2008; Fish et al. 2014; Hall et al. 2014) are programmed into the neural crest cells. Shortly after the nasal pits have formed, the facial prominences or buds of mesenchyme covered in ectoderm, grow out around the stomodeum (embryonic oral cavity). The frontonasal mass in birds and non-avian reptiles, or the medial nasal prominence in mammals, is in the center between the nasal pits, the lateral nasal prominences are lateral to the nasal pits, the maxillary prominences border the sides of the stomodeum, and the mandibular

Correspondence
Joy M. Richman, Faculty of Dentistry, Life Sciences Institute, University of British Columbia, UBC, 2350 Health Sciences Mall, Vancouver, BC V6T 1Z3, Canada. E: richman@dentistry.ubc.ca

Accepted for publication *2 February 2015*
Article published online *22 April 2015*

prominences lie inferior to the stomodeum/oral cavity (Richman & Lee, 2003).

Subsequent to outgrowth, unification of the facial prominences occurs by one of two developmental mechanisms: the 'fusion' of freely projecting prominences, in which a bilayered epithelial seam is formed as an intermediate stage (Supporting Information Fig. S1A); or the 'merging' of prominences that are separated by a deep groove (Fig. S1B) (Cox, 2004). The upper jaw derives through a complex combination of fusion and merging. The tips of the frontonasal, maxillary and lateral nasal prominences fuse (Fig. S1Ai), then form a mesenchymal bridge (Fig. S1Aii), which is followed by period of merging where cell proliferation and possibly cell migration help to fill out the remaining grooves (Fig. S1Aiii). In all amniotes, the lateral nasal and maxillary prominences are separated by a deep nasolacrimal groove, which fills in by merging (Fig. S1Bi–iii). The mandibular prominences also have a deep midline groove that merges (Jiang et al. 2006; Szabo-Rogers et al. 2010). Specific derivatives of the lateral nasal prominences are the nasal turbinates (MacDonald et al. 2004), whereas the medial nasal prominences (analogous to the frontonasal mass in birds and non-avian reptiles) form the nasal septum, premaxillary bone (Wedden, 1987; Richman & Tickle, 1989) and four incisor teeth in humans. The maxillary prominences give rise to the maxillary and palatine bones (Lee et al. 2004), whereas the mandibular prominence forms the entire mandible (Wedden, 1987; Richman & Tickle, 1989).

The facial prominences grow outwards as a result of epithelial–mesenchymal interactions (Wedden, 1987; Richman & Tickle, 1989; Richman, 1992). The communication between mesenchyme and epithelium is mediated through signaling molecules such as fibroblast growth factors (FGFs; Firnberg & Neubuser, 2002; Fuchs et al. 2010; Szabo-Rogers et al. 2008; Richman et al. 1997; Griffin et al. 2013), bone morphogenetic proteins (BMPs; Ashique et al. 2002; Abzhanov et al. 2004; Abramyan et al. 2014), endothelins (Kurihara et al. 1994; Clouthier et al. 1998; Ruest et al. 2004; Sato et al. 2008), Sonic hedgehog (Hu & Helms, 1999; Brito et al. 2006; Cobourne et al. 2009; Hu & Marcucio, 2009) and wingless-related MMTV integration sites (WNTs; Jin et al. 2012; Song et al. 2009; He et al. 2011, 2008; Reid et al. 2011). These signaling pathways regulate mesenchymal survival, proliferation, differentiation and patterning (Jiang et al. 2006; Szabo-Rogers et al. 2010).

In mammals, the fusion of the primary palate proceeds in an outward direction from the base of the outgrowing facial prominences in a 'posterior–anterior zipping-up' process (Kosaka et al. 1985). This first step results in the formation of a bilayered epithelial seam called the nasal fin between the medial nasal and lateral nasal prominences. The nasal fins eventually disappear and are replaced by mesenchymal tissue with the exception of a small posterior portion, which remains intact. This remaining portion subsequently thins out to become a fine membrane called the bucconasal membrane (also known as the oronasal membrane, or *lamina oronasalis*) (Warbrick, 1960; Gaare & Langman, 1980; Diewert & Wang, 1992; Kim et al. 2004; Som & Naidich, 2013, 2014). Shortly thereafter, the bucconasal membrane ruptures to form the connection, called the choana or internal naris, between the nasal cavities and stomodeum. The paired choanae are located in the posterior roof of the stomodeum (Parsons, 1968; Kim et al. 2004; Jiang et al. 2006; Jankowski, 2011). If the bucconasal membrane remains intact, the adult choana will be obstructed by soft tissue, bone or a combination of tissues upon maturation, resulting in a condition called choanal atresia, which affects one in 5000–10 000 people (Kim et al. 2004). Choanal atresia may also occur in combination with syndromes such as CHARGE, Apert, Crouzon and Pfeiffer (Barnett et al. 2011; Case & Mitchell, 2011; Swibel et al. 2012; Hsu et al. 2014).

Although the process of primary palate morphogenesis is superficially similar in all amniotes, the details of prominence fusion, shape and size in the embryonic cranial region may differ. One recent study has addressed the similarities and differences in superficial craniofacial morphogenesis in three-dimensional (3D) micro-CT scans of birds, non-avian reptiles and rodent, as well as reconstructed serial sections of human embryo (Young et al. 2014). Their findings suggest variation in craniofacial morphology is limited at early embryonic stages, in pre-fusion of facial prominences, but becomes much more pronounced once the primary palate is fused (Young et al. 2014). Nevertheless, comparative studies focusing on internal craniofacial structures during early embryonic development remain scarce and outdated, warranting the need for the application of 3D digital techniques that reveal the soft tissues.

Even in the chicken, a model of developmental biology and frequent model of craniofacial development, details of prominence fusion and oronasal connectivity remain poorly understood. Several early studies describe the details of the morphological progression of the developing chick embryo using either scanning electron microscopy (SEM) (Bancroft & Bellairs, 1977; Tamarin et al. 1984) or a combination of SEM with histology (Yee & Abbott, 1978; Will & Meller, 1981). With regard to the primary palate, Yee & Abbott (1978) specifically state that '... primary palate formation in the chick takes place by fusion across a continuous nasal groove...', suggesting that the oral and nasal cavities are continuous with each other during primary palate development, unlike the conditions in mammals. Will & Meller (1981), on the other hand, state that the 'rupture of the bucconasal membrane' is the important last step in a three-stage process of primary palate development in the chicken embryo. The invagination of the nasal pit (prior to the appearance of the facial prominences) is the first step and the fusion of the medial nasal and the maxillary prominences is the second step. This point of contention prompted us to revisit the question of whether all amniotes go through a conserved stage of bucconasal membrane

formation and rupture. Furthermore, previous studies of amphibians and lungfishes, which are basal to amniotes, describe them as developing a primary palate with continuously open choanae (Bertmar, 1965, 1966b). Thus, our study will allow us to determine what is the most likely basal condition for the primary palate in tetrapods.

Due to the complicated anatomy and dynamic nature of primary palate fusion, we decided to apply traditional histology, cellular dynamics in the form of apoptosis and proliferation studies, as well as a microscopic 3D digital imaging using optical projection tomography (OPT). We found that OPT was particularly powerful due to the ability to obtain surface views similar to SEM, but with the added benefit of viewing the embryos from all directions in 3D space, as well as being able to visualize epithelium and mesenchyme in digital slices in any plane of section. From these studies, we find surprising variability in the mechanism of primary palate closure within amniotes and conclude that primary palates fusion is initiated by different prominences, in a lineage-specific manner. We also show that whereas birds, turtles and lizards retain a connection between the stomodeum and nasal cavities throughout ontogeny, crocodile embryos may form their primary palate in a similar manner to mammals.

Materials and methods

Embryo acquisition, staging and fixation

All animal experiments were approved under ethics protocol #A11-0352 and were carried out at the University of British Columbia. Fertilized chicken eggs (total $n = 38$) were incubated at 38 °C and staged according to Hamburger & Hamilton (1951). Fertilized eggs from red-bellied short-necked turtle (*Emydura subglobosa,* total $n = 9$) – staged according to Werneburg et al. (2009), bearded dragon (*Pogona vitticeps*, total $n = 6$) – staged according to Dufaure & Hubert (1961), veiled chameleon (*Chamaeleo calyptratus*, total $n = 7$) – staged according to Blanc (1974), and whiptail lizard [*Aspidoscelis* (*Cnemidophorus*) *uniparens*, total $n = 9$] – staged according to Billy (1988), were donated by the Toronto Zoo. Fixed Nile crocodile embryos (*Crocodilus niloticus*, total $n = 4$)– staged according to Peterka et al. (2010), were donated by the crocodile farm in Pierrelatte (France). American alligator (*Alligator mississippiensis*, total $n = 4$) embryos were obtained from the Rockefeller Wildlife Refuge, LA, USA, and were staged according to Ferguson (1985).

Eggs were incubated in moistened vermiculite at 30 °C. Embryos were euthanized according to approved methods (injection of ~ 50–100 mL of tricaine methanesulfonate, pH 7, 5–10 min prior to removal from egg followed by decapitation). Subsequently, embryos were fixed overnight in 4% paraformaldehyde (PFA) in phosphate-buffered saline (PBS) (pH 7.4) at 4 °C.

Histological sections

After fixation, specimens were embedded in paraffin, sectioned, and stained with Picrosirius red and Alcian blue for bone and cartilage, respectively, according to Buchtova et al. (2008). E11.5 mouse (*Mus musculus, n* = 2), stage 28 chicken (*Gallus gallus*, $n = 6$), stage 4 turtle (*Emydura subglobosa*, $n = 2$), stage 12 whiptail lizard (*A. uniparens*, $n = 1$), 10-day post oviposition (dpo) crocodiles (*C. niloticus*, $n = 1$), and 15-day post oviposition (dpo) crocodiles (*C. niloticus*, $n = 2$), were sectioned into 7-μm slices and stained.

BrdU and TUNEL assay

Chicken embryos were injected with BrdU directly into the heart (50 μg per embryo). In bearded dragon, ~ 50 μg of BrdU was injected into the egg. Embryos were then fixed and embedded in paraffin and sectioned in the coronal plane. Antibody staining was carried out as described by Abramyan et al. (2014). Terminal deoxynucleotide transferase dUTP nick end labeling (TUNEL) analysis was performed with the ApopTag plus Peroxidase *in situ* Apoptosis Detection Kit detected with FITC-tagged anti-HRP (Chemicon International, Temecula, CA, USA; S7101). Images were captured using a confocal microscope (Leica Canada, Willowdale, ON, Canada; DM6000 CS). Nuclei were stained with TO-PRO3-iodide stain (diluted 1 : 5000, Life Technologies, Inc., Burlington, ON, Canada).

The percentage of proliferating or BrdU-positive cells was quantified using IMAGEJ (NIH, Bethesda, MD, USA). Chicken embryos of stages 22 ($n = 5$), 24 ($n = 5$), and 27 ($n = 6$) and one *P. vitticeps* embryo were analyzed. The percentage of proliferating cells was counted in three regions of the choanal groove/nasal cavity, 100 μm from the cavity out towards the mesenchyme in the maxillary prominence (region 1), choanal groove (region 2), and medial nasal prominence (region 3). This approach allowed us to quantify the mesenchymal proliferation pattern differences we observed in coronal sections. Factorial ANOVA followed by Fisher's LSD post-hoc testing was used to determine regions that were statistically different in their proliferation values.

OPT sample preparation, scanning and reconstruction

Embryonic heads from chicken (stage 27: $n = 6$; stage 28: $n = 6$; stage 29: $n = 4$), *E. subglobosa* (stage 2: $n = 1$; stage 3: $n = 2$; stage 4: $n = 2$; stage 5: $n = 2$), *P. vitticeps* (stage 28: $n = 1$; stage 31: $n = 2$; stage 32: $n = 2$), *C. calyptratus* (stage 33: $n = 2$; stage 34: $n = 2$; stage 35: $n = 1$; stage 37: $n = 2$), *A. uniparens* (stage 21: $n = 1$; stage 6: $n = 1$; stage 7: $n = 1$; stage 12: $n = 2$; stage 13: $n = 2$; stage 14: $n = 2$), *C. niloticus* (~ 10 dpo: $n = 1$), *A. mississippiensis* (~ stage 12, $n = 1$; ~ stage 13, $n = 2$; ~ stage 14, $n = 1$) were fixed overnight in 4% PFA/PBS (pH 7.4) at 4 °C. Subsequently, they were rinsed twice in 1× PBS. PFA or 10% formalin allows for 'autofluorescence' of tissues under the UV spectrum. Subsequently, tissues were embedded in 1% low melting point agarose and cut into blocks approximately 0.5 cm larger than the tissue sample itself. Agarose blocks encasing the tissues were then dehydrated by being placed directly into 100% MeOH and subsequently taken through five washes of 100% MeOH in the next 24 h. Afterwards, the dehydrated blocks were placed in BABB [benzyl alcohol (Sigma B-1042)/benzyl benzoate (Sigma B-6630)] in a 1 : 2 ratio. Subsequently, samples were glued to the stub and scanned in an optical projection tomography machine (model: Bioptonics 3001M) at a ~ 6–9 μm (512 × 512) resolution in the GFP1 filter. Scanned digital files were then reconstructed using NRECON (Brűker/SkyScan), reoriented using DATAVIEWER and the image stack imported into AMIRA software (FEI Visualization Sciences Group). For a subset of specimens, embryos were resliced using CTAn (SkyScan) and then exported to AMIRA software was then used for isosurface reconstruction and segmentation

of nasal cavities for generation of digital endocasts of nasal cavities. Specifically, we outlined the nasal passages in serial digital slices through the head (both in frontal and coronal planes), from the external nares until the nasal cavity ended (as in mouse) or until the nasal cavities opened into the oral cavity (as in chicken). By starting from the middle of the nasal cavity and going outward in each direction, this method allowed us to perform an unbiased analysis of the extent of the nasal cavities to assess if the choanae and the external nares were open or closed.

Results

OPT reconstructions are sufficiently high resolution to visualize the point of initial contact in the fusing primary palate

Using OPT, we obtained digital reconstructions of the head and nasal cavities of embryonic E.11.5 mouse (*M. musculus*), ~ 10 dpo (~ 166 mg) crocodile (*C. niloticus*), stage 28 chicken (*G. gallus*) as well as stage 4 turtle (*E. subglobosa*) (Fig. 1). We define approximately equivalent stages based on the presence of grooves between lateral nasal and maxillary prominences (nasolacrimal groove) as well as between the frontonasal mass and maxillary prominences. The process of merging between the frontonasal mass and maxillary prominences/lateral nasal prominences is still incomplete and thus the furrows or grooves are visible (Fig. 1A-D). The initial point of contact during lip fusion relative to the nasolacrimal groove varies according to taxon. In the mouse and crocodile embryos, the fusion zone is in line with the nasolacrimal groove, with the majority of the initial fusion being between the medial and lateral nasal prominences (Fig. 1A,B). In the stage 28 chicken, however, the nasolacrimal groove is superior to the point of fusion between the frontonasal mass and maxillary prominence. In chicken, unlike in mouse and crocodile, there is no participation of the lateral nasal prominence during the initiation of primary palate fusion (Fig. 1C). Conversely, in the turtle, we observe fusion of the frontonasal mass with the lateral nasal prominence, at a more superior position than in crocodile and mouse (Fig. 1D). Despite the unified mesenchyme in the maxillary and lateral nasal prominences, Patterson et al. (1984) and McGonnell et al. (1998) report that labeled cell populations within each prominence do not mix with each other. Thus, the specific prominences involved in the initiation of primary palate fusion may influence susceptibility to orofacial clefting.

We used the virtual sections to determine whether the nasal passages had opened posteriorly into the oral cavity. We confirmed that in all embryos, the lateral corners of the frontonasal mass (globular processes of His; Som & Naidich, 2013) have recently fused, as shown by the bilayered epithelial seam between the lateral nasal prominence and/or the maxillary prominence (Fig. 1A′,B′,C′,D′). In posterior sections, mouse and crocodile had no posterior opening, instead there was a blunt end to the nasal passages (Fig. 1A″, B″), whereas in chicken and turtle there is a gap between the frontonasal mass and maxillary prominences in the region of the choana (Fig. 1C″,D″).

Next we examined representative animals from three distinct families of lizards: Teiidae (whiptail lizard, *A. uniparens*), Chamaeleonidae (veiled chameleon, *C. calyptratus*), and Agamidae (bearded dragon, *P. vitticeps*). In all three species, we observed fusion between the lateral nasal prominences and the frontonasal mass, similar to mouse, crocodile and turtle (Fig. 2A-C). Interestingly, the lateral nasal prominences completely fused with the frontonasal mass, temporarily closing off the external nares and isolating a portion of the nasal cavity (Fig. 2D,D′,E,E′,F). This phenomenon can also be clearly observed in endocasts of the veiled chameleon (Fig. 3D′) and the bearded dragon (Fig. 2E′), where no external communication is visible and the cavity extend behind the fused external nares. In digital sections (coronal plane), however, of the upper nasal cavities of chameleon, bearded dragon and whiptail lizard, the prominences are clearly fused, whereas the nasal cavity can be observed as openings behind the fusion zone in bearded dragon and chameleon (Fig. 2G,H) and as fused, bilayered epithelia in the whiptail lizard (Fig. 2I).

Histological analysis concurs with OPT virtual sections

Once we identified the individual prominences involved in primary palate and nasal cavity formation in each lineage, we used these fine external features such as the presence of the nasolacrimal groove and recent fusion of the maxillary and medial nasal prominences, to ensure embryos were at equivalent stages. We complemented real histology with virtual histology and 3D scans of the head to ensure that we would capture the bucconasal membrane if present. We only observed bucconasal membranes in the posterior of the nasal cavities in the E11.5 mouse embryo (Fig. 3A-C, black and white arrowheads). Equivalent sections in chicken, turtle and lizard showed connections between the oral and nasal cavities (Fig. 3D,E,F, respectively), suggesting that a bucconasal membrane does not form.

Unlike other reptiles, in the crocodile embryos, the nasal cavities appear separated from the stomodeum during primary palate formation at 10 dpo (~ 160 mg, Fig. 1B′,B″). Histological analysis of a different 10 dpo (~ 160 mg) crocodile embryo reveals a substantial nasal fin between the lateral and medial nasal prominences (Fig. 3G), similar to the nasal fin in mammals. We have therefore captured the stage just after fusion of the tips of the facial prominences. In other words, the embryos are past the point of invagination of the nasal pit which occurs after nasal placode induction. If the embryo was at the earlier stage of nasal pit invagination, there would be continuous mesenchyme around the nasal pit space, as exhibited in section of the 10 dpo crocodile posterior to the nasal fin (Fig. 3H).

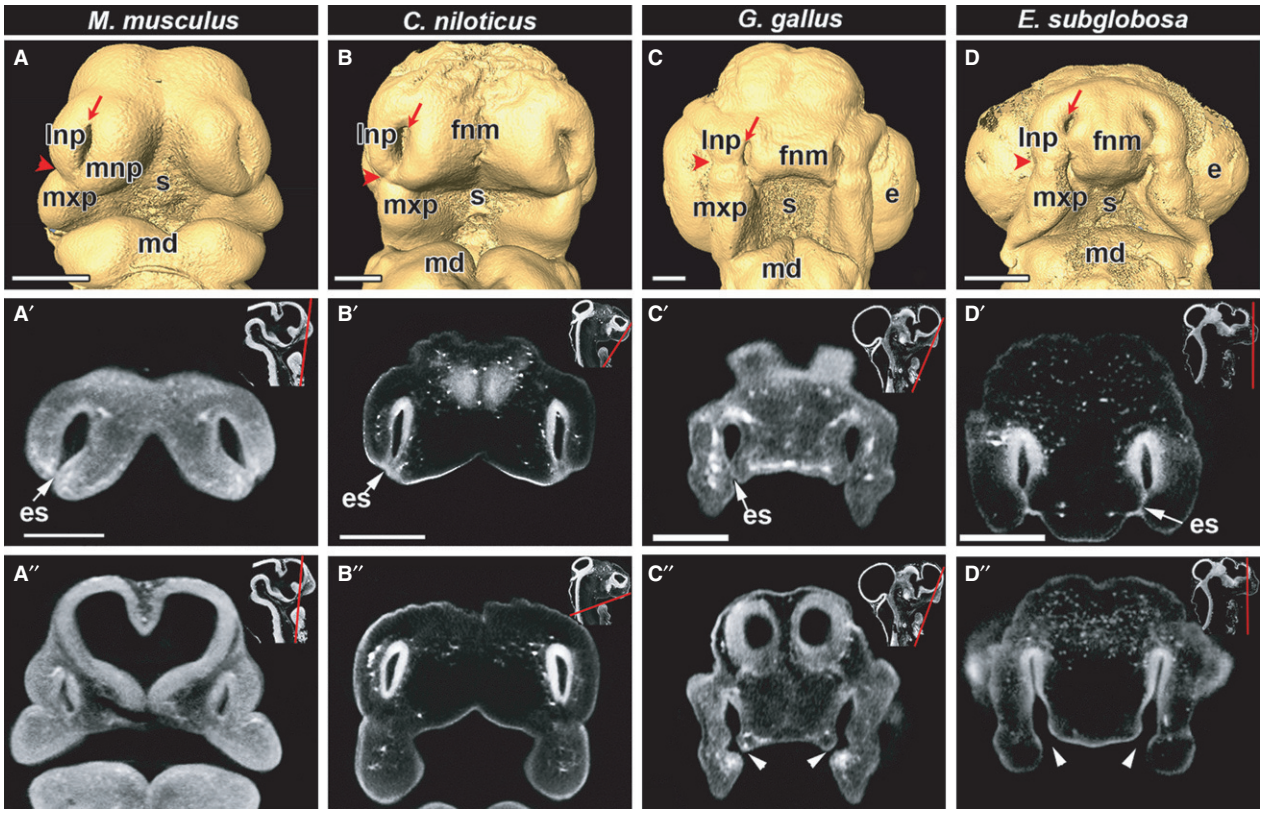

Fig. 1 Primary palate initiation in amniotes documented with OPT scanning. Frontal views of isosurfaces created in AMIRA (A-D) and virtual OPT slices (A′-D″) of embryos are shown for E11.5 mouse (*Mus musculus*), ~ 10-day crocodile (*Crocodilus niloticus*), stage 28 chicken (*Gallus gallus*) and stage 4 turtle (*Emydura subglobosa*). All embryos have open external nares (red arrows with tails in A-D). The nasolacrimal groove which separates the lateral nasal prominence from the maxillary prominence (red arrowheads in A-D) is used as a reference landmark to compare the site of initial fusion between facial prominences. In the mouse and crocodile embryos (A,B), fusion occurs jointly between the lateral nasal, medial nasal and maxillary prominences and the fusion point is approximately at the level of the nasolacrimal groove. In the chicken embryo (C) fusion begins between the frontonasal mass and the maxillary prominence inferior to the nasolacrimal groove. In the turtle (D), fusion initiates between the frontonasal mass and the lateral nasal prominence and the fusion zone is superior to the nasolacrimal groove. Optical sections in the anterior frontal plane show that the tips of the prominences are fused in all specimens, as demonstrated by the presence of a bilayered epithelial seam (A′,B′, C′,D′; white arrow), whereas posterior sections show closed choanae in mouse and crocodile and open choanae in the chicken and turtle (A″,B″,C ″,D″; white arrowheads). Insets show the plane of section with a red line (A′,A″,B′,B″,C′,C′,D′,D″). Key: e, eye; es, epithelial seam; fnm, frontonasal mass; lnp, lateral nasal prominence; md, mandibular prominence; mnp, medial nasal prominence; mxp, maxillary prominence; s, stomodeum. Scale bars: 500 μm.

Histological analysis of crocodile embryos at a slightly older stage (15 dpo; 400 mg) revealed that the choanae do open up later in development (Supporting Information Video S1). Despite identifying the stage of primary palate fusion in crocodile, we did not identify a bucconasal membrane *per se*. Further sampling of embryos between 10 and 15 dpo would be necessary to determine whether a transient bucconasal membrane exists in crocodiles.

The data thus far suggested that open choanae were found in most avian and non-avian reptiles. However, the bucconasal membrane is so small that it is possible that it could have been missed in histological analysis. We next wanted to take advantage of the 3D OPT image stacks to determine whether there was a communication between the oral and nasal cavities.

Nasal cavities in 3D

Here we created 3D endocasts of the nasal cavities by segmenting out the spaces between the epithelia on serial virtual sections (Fig. 4A-F″). The external nares were open and the nasal cavities were visible in all of the specimens (Fig. 4A-E″) with the exception of the *A. uniparens* (Figs 2C, F,I and 4F-F″). In mouse (Fig. 4A-A″; Supporting Information Fig. S3F) and young crocodilian (10 dpo crocodile, Figs 4B-B ″, S2A-D and S3G), the segmented nasal passages formed a blunt end at their deepest point and did not connect to the oral cavity. As mentioned previously, the collected crocodile embryos may have bracketed the stage when a bucconasal membrane was present. We therefore obtained alligator embryos of an intermediate stage (stage 12, 13; Ferguson,

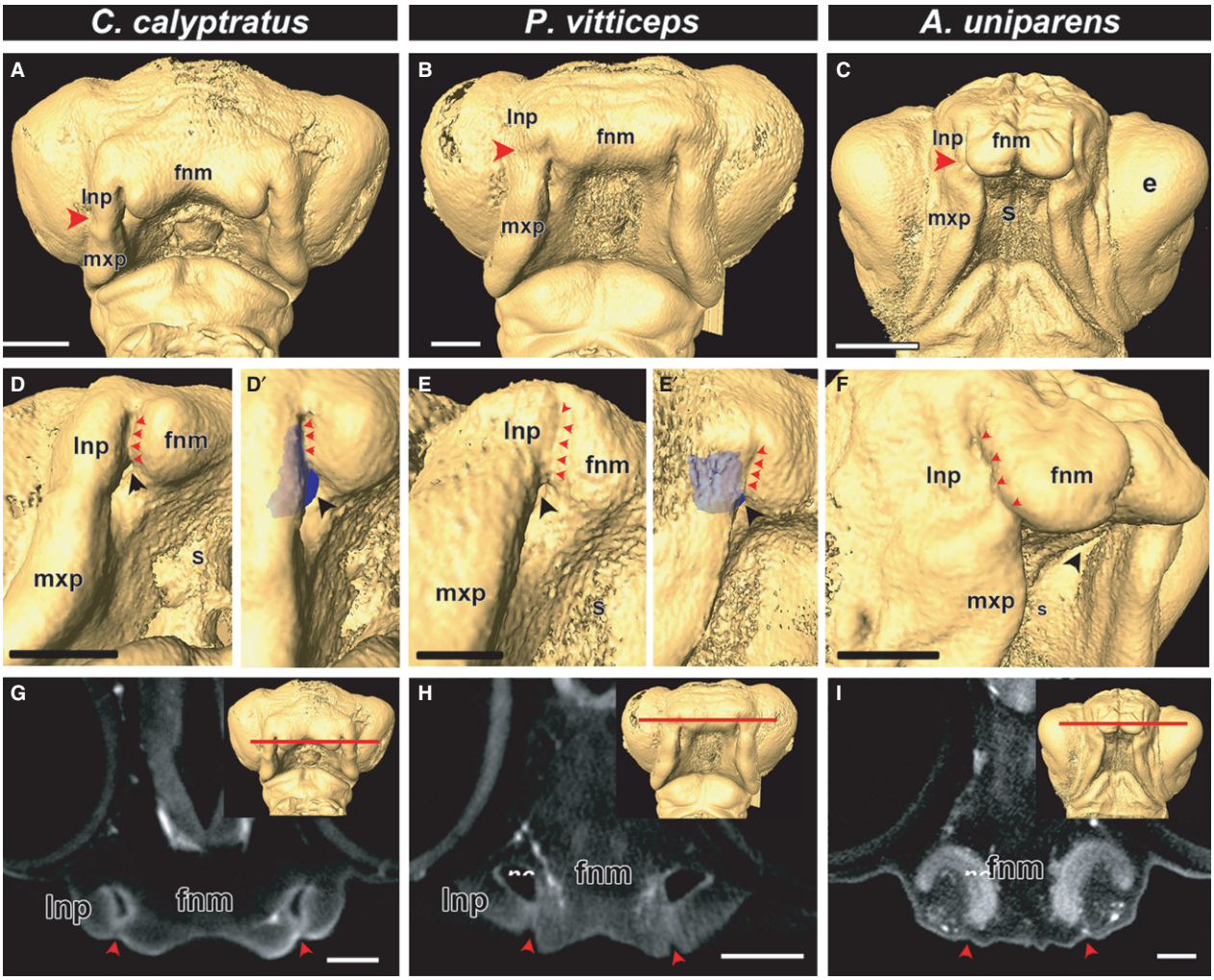

Fig. 2 Comparison of fusion in lizard embryos. Isosurfaces of stage 34 chameleon (*Chamaeleo calyptratus*), stage 31 bearded dragon (*Pogona vitticeps*) and stage 12 whiptail lizard (*Aspidoscelis uniparens*). Based on the position of the nasolacrimal groove (A-C; red arrowheads), primary palate development is initiated by the fusion of the frontonasal mass with the lateral nasal prominence. A closer view of the fusion zone reveals complete fusion of the lateral nasal prominence and the frontonasal mass, completely closing off the external nares (D,D′,E,E′,F; red arrowheads). An endocast of the nasal cavity (blue) reveals that it lies behind the fusion zone (D′,E′). Virtual coronal sections in the plane of the fusion zone (G, H,I; red line in the inset) reveals that the prominences are indeed fused to each other (G,H,I; red arrowheads) and there is an open cavity (the nasal cavity) directly behind the fused prominences. Key: e, eye; fnm, frontonasal mass; lnp, lateral nasal prominence; mxp, maxillary prominence; nc, nasal cavity; s, stomodeum. Scale bars: 500 μm.

1985). We gauge the stage 12 alligator to be slightly older than the 10-day crocodile embryo based on the decreased separation of the nasal pits, the shallower depth of the midline frontonasal furrow and the increased size of the eyes. The alligators had a fully connected oral and nasal passage at stage 12 and 13 (Figs 4C-C″, S2E–P and S3H).

Chicken, turtle and lizard all demonstrated endocasts that open into the stomodeum (Figs 4D-F″ and S3A–E). These segmented nasal volumes confirmed that we had not missed the presence of a membrane deeper in the nasal cavity (Supporting Information Videos S2 and S3 of chicken). The presence of a membrane would have resulted in a gap in the reconstructed structure. Thus, whereas chicken, turtle and lizard form open choanae at initiation of primary palate fusion, crocodilians may go through a closed choana phase, which connects later in development through an as yet unknown mechanism.

Cellular dynamics in avian choanal groove

Due to the similarity of the open choana in chicken and several non-avian reptiles, and because the chicken is accessible for experimental manipulation, we explored the cellular dynamics involved in choana formation in the avian embryo. Although there is a significant amount of growth occurring in the facial prominences, the choanal groove remains as a depression instead of filling in and closing off the nasal cavity from the stomodeum. We

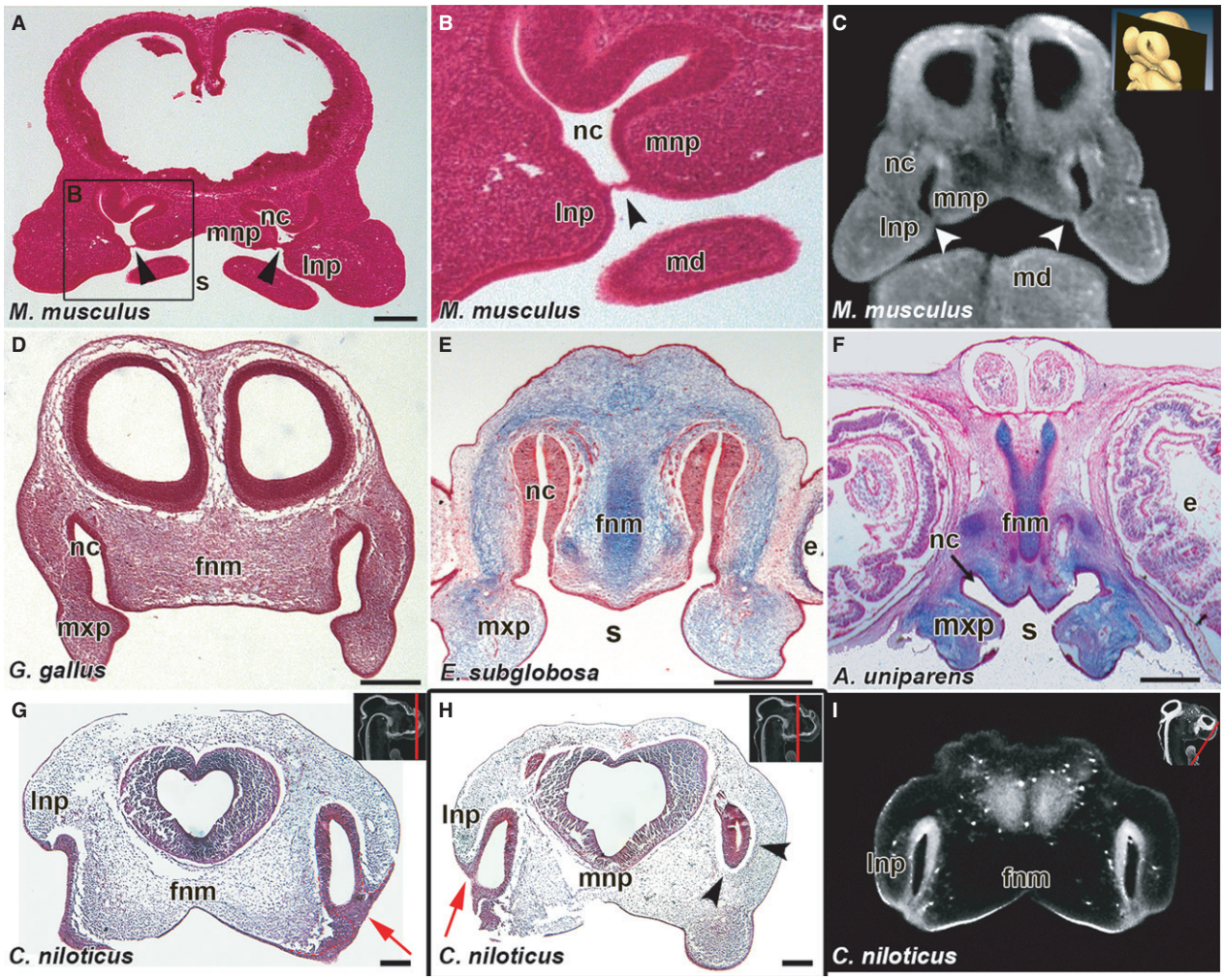

Fig. 3 Bucconasal membrane is only present in the mouse. Histological sections in the frontal plane from E11.5 mouse (*Mus musculus*) (A,B) and virtual section of E11.5 mouse (C), show the bucconasal membrane closing off the choanae from the stomodeum (black arrowheads in A, B; white arrowheads in C). In stage 28 chicken (*Gallus gallus*) (D), stage 4 turtle (*Emydura subglobosa*) (E) and stage 12 whiptail lizard (*Aspidoscelis uniparens*) (F) there is a continuous connection between the nasal cavity and the stomodeum via open choanae. *Crocodilus niloticus* embryo shows fused lateral and medial nasal prominences externally with an epithelial plug in between (red arrows, G,H). Posterior section reveals the region past the nasal fin on the left side of the head where mesenchyme surrounds the nasal cavity (H, arrowheads). Virtual Frontal section from OPT scan of 10-day crocodile embryo revealing fusion regions between the lateral nasal prominence and the frontonasal mass (I). Key: e, eye; fnm, frontonasal mass; lnp, lateral nasal prominence; mnp, medial nasal prominence; nc, nasal cavity; s, stomodeum. Scale bars: 250 μm (A); 200 μm (D-H).

hypothesized that there are two methods by which this can occur: (i) mesenchymal apoptosis allowing the choanal groove to invaginate in a posterior direction while the prominences are proliferating anteriorly or (ii) differential proliferation alone is driving the prominences forward while the choanal groove remains behind, with no apoptotic factors involved.

We analyzed proliferation in the lowest plane of section in which we could still observe the frontonasal mass (Fig. 5B). Three mesenchymal regions were analyzed for proliferation at different stages of development, including the cranial end of the maxillary prominence (Region 1), the region posterior to the choanal groove (Region 2) and the lateral frontonasal mass (Region 3) (Fig. 5C). At stages 22 and 24, early in nasal cavity establishment and before choanal groove formation, there is no variation in proliferation patterns between the three regions (Fig. 5D). Also, we observed approximately the same percentage of proliferation in all regions at both stages, indicating a steady rate of proliferation in the mesenchyme immediately surrounding the nasal cavity. However, at stage 27, we observed a relative decrease in proliferation in the mesenchyme of the choanal groove compared with the lateral nasal and frontonasal masses, which maintain levels of proliferation similar to younger stages (Fig. 5D; Supporting Information Table S1). This pattern of proliferation gradient was qualita-

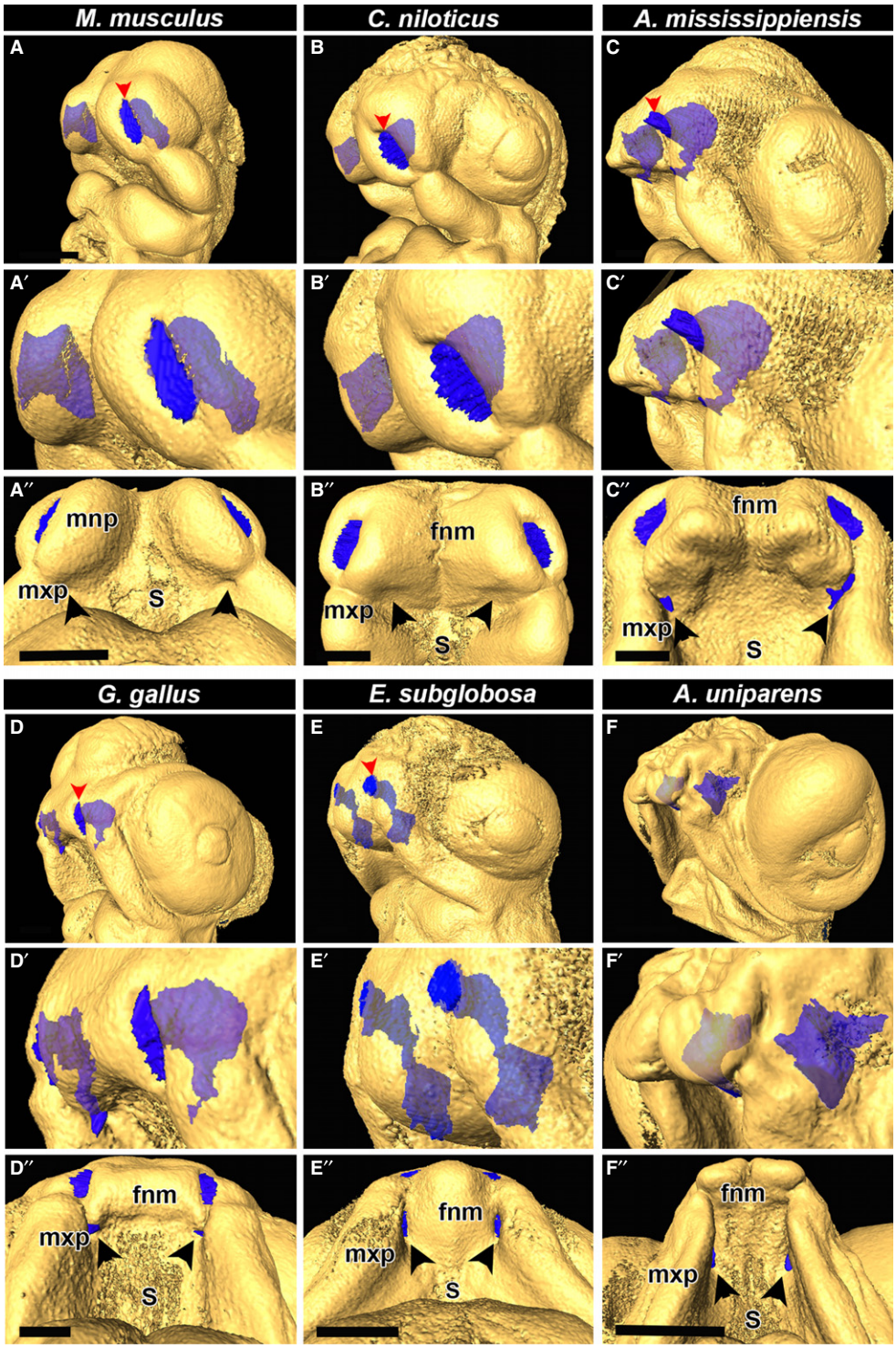

Fig. 4 Endocasts of nasal cavities illustrate variation in choana formation between mammals as well as all major reptilian lineages, including birds. Rotational views of nasal cavities in E11.5 mouse (*Mus musculus*), ~ 10-day crocodile (*Crocodilus niloticus*), stage 12 alligator (*Alligator mississippiensis*), stage 28 chicken (*Gallus gallus*), stage 4 turtle (*Emydura subglobosa*) and stage 12 whiptail lizard (A-F). Endocasts of nasal cavities in mouse and young crocodile, alligator, chicken and turtle show the nasal cavities open to the external nares (darker blue colour, red arrowheads, A,A′,B, B′,C,C′,D,D′,E,E′). The external nares in the lizard is fused (as shown in Fig. 2) and does not open until later in development (F-F′). In the mouse and crocodile there is a blind sac in the posterior of the nasal cavity (A′,A″,B′,B″). In the older alligator, chicken turtle and lizard, the nasal cavities have connected with the oral cavity, indicating an open choana (C, C′,D′,D″,E′,D″,F′,F″). Key: fnm, frontonasal mass; mnp, medial nasal prominence, mxp, maxillary prominence; s, stomodeum. Scale bars: 500 μm.

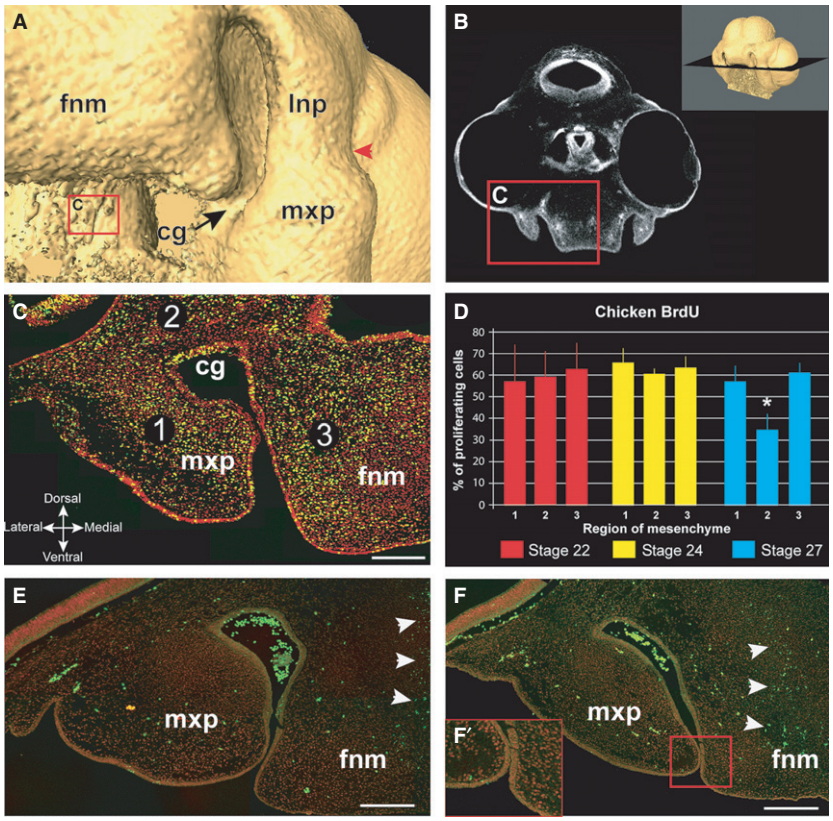

Fig. 5 BrdU labeling in chicken embryos at the time of choana formation. A stage 27 embryo shows the opening between nasal and oral cavities (A). The coronal plane of section for BrdU cell counts passes through the choanal groove (B). (C) A representative section that passes through the maxillary prominence and frontonasal mass. Mesenchymal nuclei are labeled in red, BrdU-labeled cells are yellow. Percentage proliferating cells was calculated in three regions of mesenchyme (C); region 1 – maxillary prominence; region 2 – the base of the choanal groove; region 3 – the lateral edge of the frontonasal mass. At stage 22 and 24, where the choanal groove has not formed yet, there is no significant difference in proliferation among the three regions. However, at stage 27 there is a significant decrease in proliferation in region 2 (asterisk, $P < 0.005$) compared with the other regions, where proliferation rates remain approximately the same as in stages 22 and 24 (~ 60%) (D). TUNEL analysis on stage 27 (E) and stage 28 (F) reveals minimal apoptosis in both the mesenchyme of the choanal groove (red arrowheads) as well as the fusion zone between the prominences (F′). The only region with significant apoptosis was the middle of the frontonasal prominence, where the nasal cartilage will form (white arrowheads). Key: cg, choanal groove; fnm, frontonasal mass; lnp, lateral nasal prominence; mxp, maxillary prominence, Scale bars: 100 μm (C,E,F).

tively observed in a stage 31 *P. vitticeps* embryo, consistent with a shared mode of choanal groove formation/facial prominence extension in birds and non-avian reptiles (Supporting Information Fig. S4).

We subsequently checked whether the drop in proliferation is accompanied by an increase in apoptosis and found minimal apoptosis in all of the three regions of embryos both before fusion (stage 27; Fig. 5E) and after fusion (stage 28; Fig. 5F) of maxillary and frontonasal prominences. There were, however, numerous apoptotic cells towards the center of the frontonasal mass, where chondrogenesis is taking place. This is similar to the results reported by other studies (McGonnell et al. 1998; MacDonald et al. 2004). Our detection of this apoptotic region serves as a positive control. Thus the pattern of differential proliferation is the likely mechanism by which the choanal groove deepens while the medial nasal and maxillary prominences grow out and fuse around the groove.

Discussion

Primary palate development is common to all amniotes and this study has identified differences in the specific prominences which initiate fusion of the primary palate, depending on the Order of the animals we examined. There is a surprising degree of plasticity with respect to the specific prominences involved in lip fusion. It is possible that the variation in initial contact correlates with later beak or jaw shape. Furthermore, during and after the fusion of the primary palate, we found that most reptiles (including birds), with the sole exception of the crocodile, maintain a persistent connection between the oral and nasal cavities via an open choanae. This key difference in most of the nonavian reptiles and birds eliminates the requirement of the precarious process of bucconasal membrane rupture, which, if incomplete, can lead to birth defects such as choanal atresia, as well as respiratory distress, in neonate mammals. Further-

more, through studies of proliferation and apoptosis patterns in avian facial prominences, we identified a proliferation gradient which allows the choanae to persist as open cavities in reptiles, while prominences grow out and fuse with each other to form the primary palate.

Inter-species differences in the prominences initiating fusion of the primary palate

The exact sequence of events leading to the fusion of the prominences to form the primary palate in amniotes is still a contentious topic in the scientific community (Jiang et al. 2006; Song et al. 2009). Within mammals, most studies agree that in the mouse primary palate, the medial and lateral nasal prominences fuse first and are subsequently joined by the maxillary prominence (Trasler, 1968; Gaare & Langman, 1980; Diewert & Wang, 1992; Gong & Guo, 2003; Kim et al. 2004). We also found this sequence to be true using OPT scans of mouse embryos. In human, Diewert & Wang (1992) report that at 37 days post fertilization (Carnegie stage 16), the medial nasal prominences make initial contact with the maxillary prominence, similar to the chicken embryo. Subsequently, at early stage 17, the area of contact spreads to include the lateral nasal prominence. This disparity, even within mammals, indicates there are many paths to achieving lip fusion.

Surprisingly, we found that crocodile primary palate formation/fusion is remarkably similar to that of mammals, complete with nasal fin formation and initial separation of the oral and nasal cavities. However, in slightly older crocodilians (both crocodile and alligator embryos) the choanae were open. Both alligators and crocodiles are similar in terms of their point of initial contact (Ferguson, 1981; Peterka et al. 2010) but denser sampling of the key stages would be necessary to answer the question of true bucconasal membrane formation in crocodilians.

Recently, Young et al. (2014) performed an extensive study of the primary palate using externally placed landmarks followed by geometric morphometrics to assess developmental morphospace for a large variety of amniotes. They found that all amniotes share reduced shape variance and convergent growth during the period spanning the period of facial prominence outgrowth through fusion of the primary palate. After fusion, phenotypic variation increases significantly to facilitate the diversity in shapes of adult animals. Furthermore, through *in vivo* experiments on chicken embryos, they found that deviation from this early, conserved trajectory of craniofacial development results in a mismatch of the shapes and sizes of prominences, resulting in a cleft. Thus, the threat of clefting likely dictates a strong intolerance of morphological change during primary palate development.

However, in the study by Young et al. (2014), the authors did not differentiate between the lateral nasal and maxillary prominences, instead presenting this region as a combined 'maxillary component' which fuses with frontonasal prominence. In contrast, our results show that the maxillary or lateral nasal prominence can be involved in the initiation of primary palate fusion independently of each other. Taken together, with the previous study (Young et al. 2014), we propose that delegating the initiation of fusion to only two of the prominences allows for the 'free' prominence to tolerate more variance in shape and size while still permitting the primary palate to fuse normally. This separation of jobs adds another dimension of putative variability to the morphospace, in an otherwise strict and conservative system intolerant of any major changes.

Contrasting mechanisms of choana formation in reptiles and mice

Although all amniotes pass through a conserved stage of primary palate fusion (Fig. S5A,B,C), there is a decision point that occurs prior to fusion as to whether the choanal is completely closed off, separating and oral and nasal cavities (Supporting Information Fig. S5D), or whether this intervening region is retained as a concavity, forming an open choana (Fig. S5E). If an open choana is to form, differential proliferation around the nasal pit correlates with formation of the choanal groove (Fig. S5α). Our data show that there are minimal differences in proliferation in the lateral nasal and frontonasal mass mesenchyme between stages 22 and 27, a period of great morphogenetic change. However, in the mesenchyme at the base of the nasal pit there is a striking decline in proliferation specifically at stage 27. Our work agrees with that of a previous study focused on nasal pit morphogenesis in the chicken embryo (Minkoff & Kuntz, 1977). Those authors concluded that deepening of the nasal passages was not due to greatly increased proliferation in the frontonasal mass and lateral nasal prominence but rather to the steep drop-off in proliferation of the mesenchyme basal to the nasal pit, especially between stages 25 and 27. Thus the same proliferation differences contribute to both choanal groove formation and nasal passage invagination.

We wondered whether mammals also have differential proliferation patterns around the nasal cavity to help to define the choana. Several studies have described higher proliferation in the distal ends of the outgrowing prominences (near the putative zone of fusion/nasal fin formation) and lower proliferation in the mesenchyme at the cranial end of the outgrowing prominences (Diewert & Wang, 1992; Gui et al. 1993; Iamaroon et al. 1996; Jin et al. 2012). However, these authors did not focus on coronal sections in which the facial prominences and the mesenchyme dorsal to the nasal cavity are captured in the same plane. It is also necessary to compare proliferation at several stages to measure whether the facial prominence proliferation is maintained at a similar level, while there is lower proliferation close to the choana.

In the mouse there is significant apoptosis in the fusion zone of the lateral nasal and medial nasal prominences (Jiang et al. 2006) but no one has studied whether the bucconasal membrane has increased levels of programmed cell death prior to rupture. Here we excluded apoptosis from playing a role in choanal groove formation in the avian reptile. The lack of involvement of apoptosis in choanal groove formation applies to other non-avian reptiles. In a previous study from our group in which the turtle embryo was studied specifically in the region of the choana (Abramyan et al. 2014), we found minimal apoptosis in the mesenchyme adjacent to the nasal cavities and choanae. Thus, we can conclude that the mechanism of choanal groove formation in avian and non-avian reptiles does not involve apoptosis. Instead it is a differential decrease in proliferation in adjacent mesenchyme that is the most likely mechanism (Fig. S5).

FGF and RA signaling are candidate pathways involved in choana formation

There are two prime candidate signaling pathways that could be involved in choana formation. The FGF pathway has been shown by our group (Szabo-Rogers et al. 2008) to regulate differential proliferation around the nasal pit in the chicken embryo at stage 26–27, the same stages as studied in the present paper. A bead soaked in an antagonist for FGF receptors was placed into a region equivalent to zone 3 used here. The bead implant caused a significant decrease in proliferation and ultimately caused clefts (Szabo-Rogers et al. 2008). Thus we realize that it was the disruption of the differential proliferation between zones 2 and 3 that was the cause of the clefts in that study. In addition to differential proliferation, the FGF pathway has been linked to human choana formation. Mutations in FGFR3 cause a specific form of craniosynostosis in which the majority of patients also have choanal atresia (Crouzon syndrome with acanthosis nigricans, OMIM #612247) (Schweitzer et al. 2001). In mammals, *Fgf8* is specifically expressed in the nasal fin, which forms the bucconasal membrane (Dupe et al. 2003), so any disruption in FGF signaling in the membrane could affect cell survival or proliferation. The cellular dynamics taking place during bucconasal membrane formation and rupture have not yet been studied.

Another candidate molecule that could play a role specifically in bucconasal membrane rupture is retinoic acid. The enzyme that synthesizes retinoic acid, *Raldh3,* is expressed specifically in the nasal fin and nasal epithelium in the mouse embryo (Dupe et al. 2003; Song et al. 2009; Jin et al. 2012). Importantly, when *Raldh3* was targeted in mice the main phenotype was fully penetrant choanal atresia accompanied by a persistent nasal fin expressing *Fgf8* (Dupe et al. 2003). The addition of exogenous RA to the pregnant dams rescued the choanal atresia phenotype in the majority of animals. Thus a certain level of RA signaling is clearly necessary for the breakdown of the bucconasal membrane in the mouse. The exact mechanism by which the bucconasal membrane persisted was not examined in that study; however, it was clear that the epithelium of the nasal fin was present longer than it would have been normally.

Implications for selecting a model organism to study cleft lip and choanal atresia

Studies such as ours can aid in identifying a proper model organism for specific defects in primary palate formation. For example, all animals examined would be good models for lip formation but the best of these is actually the chicken, since it most resembles human in terms of the contact of facial prominences during lip fusion. Indeed, the chicken embryo can be induced to form a notch in the side of the upper beak not unlike human cleft lip (Ashique et al. 2002; Song et al. 2004; Szabo-Rogers et al. 2008; Higashihori et al. 2010). On the other hand, the chicken is not an appropriate model for studying choanal atresia due to the lack of a bucconasal membrane. However, it is possible that crocodilians could be an interesting comparison with mammals since they appear to form a transient separation between the oral and nasal cavities.

The basal condition for the primary palate in tetrapods is a choanal groove

The olfactory and respiratory organs of the most basal vertebrates is thought to be separated, as in the lamprey (Parsons, 1971; Jankowski, 2011; Oisi et al. 2013), where the olfactory organ is a blind pouch through which water is irrigated, and respiration occurs through swallowing of water and irrigation of the brachia. Exaptation of the olfactory organ to a respiratory role may explain the fusion of the aforementioned organs into a single olfactory and respiratory organ observed in more derived lineages such as Dipnoi (subclass of lobe-finned, air-breathing, freshwater fishes such as the Australian lungfish, *Neocerotodus fosteri*) and hagfish, as well as amphibians such as the salamander (Bertmar, 1965, 1969; Oisi et al. 2013). Basal vertebrates such as amphibians and lungfishes do not form a bucconasal membrane during embryogenesis (Bertmar, 1965, 1966a,b, 1969; Jankowski, 2011) (Fig. 6).

The development of this 'novel' combined olfactory and respiratory organ in basal vertebrates is described in great detail by several authors in early to mid-20th century studies (Allis, 1917, 1932; Parsons, 1959, 1971; Bertmar, 1965, 1966a,b, 1969; Panchen, 1967). Although their primary studies focused on fishes, both Allis and Bertmar refer to a 'naso-buccal groove' being present in all basal vertebrates. This groove is likely analogous to the choanal groove that we describe in our study. Bertmar (1965) specifically describes the naso-buccal groove as a 'larval' structure running caudally from the primary nasal opening and ending in the stomodeum. He subsequently describes the forma-

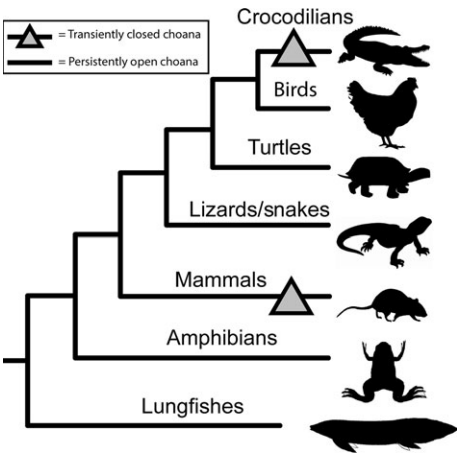

Fig. 6 A cladogram depicting the phylogenetic relationships of the major tetrapod vertebrate lineages. A triangle labels the putatively closed choanae in crocodilians and mammalians. Due to their distant phylogenetic relationship, the most parsimonious conclusion leads to two independent derivations of closed choanae, once in mammals and once in crocodilians. Additionally, the open choana formation is the likely ancestral condition in amniotes, since basal (non-amniote) lineages such as lungfishes and amphibians also develop open choanae.

tion of a 'nasal bridge', which is formed from the fusion of the epithelial edges of the naso-buccal groove, between the anterior and posterior nostrils. The nasal bridge is analogous to the bridge formed over the choanal groove from the fusion of the frontonasal mass and maxillary prominence we describe in chicken, as well the fusion of the medial and lateral nasal prominences in turtles, leaving both external and internal nares open.

Interestingly, in yet another deviation involving the formation of the choanae, Bertmar (1966a), studying salamander (*Hynobius retardatus*), found that Urodele amphibians do not form their choanal tubes and choanae via naso-buccal grooves but instead from three portions, including the gut process. Despite this deviation in extant urodeles, he does state that a persistent naso-buccal groove extending from the olfactory organ to the choanae in the buccal cavity is the likely ancestral state for these amphibians (Bertmar, 1966b). Both Bertmar and Panchen agree that it is likely that the naso-buccal groove is common to all gnathostomes as an embryological structure (Bertmar, 1966b; Panchen, 1967). Thus we conclude that birds, lizards and turtles have likely retained the ancestral mode of open choana formation, whereas the formation of a transiently closed choana represents a derived trait (Fig. 6). The exception to this appears to be the crocodilians. Due to limitations of our sample set we cannot distinguish between the possibilities that crocodilians form closed choanae which subsequently open through bucconasal membrane rupture like in mammals, or that a choana groove forms after the initial fusion. Interestingly, crocodilians are also the only reptiles that have a complete secondary palate similar to mammals (Ferguson, 1981). This intriguing link between primary and secondary palate development in crocodilians will be the subject of future studies.

In summary, our study has provided new insights into the mode of fusion of the primary palate, the temporal and spatial differences in cell proliferation that explain the deepening of the choanal groove, and the evolution of the choana in tetrapods, and has also helped to clarify the most appropriate model organisms in which to study development of these structures.

Acknowledgements

This work was funded by an NSERC discovery grant #326908 and a CIHR operating grant #MOP-123536 to J.M.R. J.A. is a recipient of an NIH *Ruth L. Kirschstein NRSA* Postdoctoral Fellowship (award no.: 1F32 DE022999-03). The authors are grateful to the Ferme aux crocodiles, Pierrelatte, France, for providing the crocodile embryos and Dr. Theresa Grieco for insightful discussions on embryonic morphology. We would additionally like to thank Ruth Elsey of the Rockefeller Wildlife Refuge for alligator embryos. The authors declare no conflict of interest.

Author contributions

J.A. – contribution to concept and design, acquisition of data, data analysis/interpretation, drafting of manuscript, critical revision of manuscript, approval of article. B.T.P. – acquisition of data, critical revision of manuscript, approval of article. J.M.R – data analysis/interpretation, critical revision of manuscript, approval of article.

References

Abramyan J, Leung KJ, Richman JM (2014) Divergent palate morphology in turtles and birds correlates with differences in proliferation and BMP2 expression during embryonic development. *J Exp Zool B Mol Dev Evol* **322**, 73–85.

Abzhanov A, Protas M, Grant BR, et al. (2004) Bmp4 and morphological variation of beaks in Darwin's finches. *Science* **305**, 1462–1465.

Allis EP (1917) The lips and the nasal apertures in the gnathostome fishes, and their homologues in the higher vertebrates. *Proc Natl Acad Sci U S A* **3**, 73–78.

Allis EP (1932) Concerning the nasal apertures, the lachrymal canal and the bucco-pharyngeal upper lip. *J Anat* **66**, 650–658.

Ashique AM, Fu K, Richman JM (2002) Endogenous bone morphogenetic proteins regulate outgrowth and epithelial survival during avian lip fusion. *Development* **129**, 4647–4660.

Bancroft M, Bellairs R (1977) Placodes of the chick embryo studied by SEM. *Anat Embryol (Berl)* **151**, 97–108.

Barnett S, Moloney C, Bingham R (2011) Perioperative complications in children with Apert syndrome: a review of 509 anesthetics. *Paediatr Anaesth* **21**, 72–77.

Benton MJ (1990) Phylogeny of the major tetrapod groups: morphological data and divergence dates. *J Mol Evol* **30**, 409–424.

Bertmar G (1965) The olfactory organ and upper lips in dipnoi. An embryological study. *Acta Zool* **46**, 1–40.

Bertmar G (1966a) The development of skeleton, blood vessels and nerves in the dipnoan snout, with a discussion on the homology of the dipnoan posterior nostrils. *Acta Zool* **47**, 88–150.

Bertmar G (1966b) On the ontogeny and homology of the choanal tubes and choanae in urodela. *Acta Zool*, **47**, 81–150.

Bertmar G (1969) The vertebrate nose, remarks on its structural and functional adaptation and evolution. *Evolution* **23**, 131–152.

Billy AJ (1988) Observations on the embryology of the unisexual lizard *Cnemidophorus uniparens* (Teiidae). *J Zool Lond* **215**, 55–81.

Blanc F (1974) Table de développement de *Chamaeleo lateralis* Gray, 1831. *Ann Embryol Morphol* **7**, 99–115.

Brito JM, Teillet MA, Le Douarin NM (2006) An early role for sonic hedgehog from foregut endoderm in jaw development: ensuring neural crest cell survival. *Proc Natl Acad Sci U S A* **103**, 11607–11612.

Buchtova M, Handrigan GR, Tucker AS, et al. (2008) Initiation and patterning of the snake dentition are dependent on Sonic hedgehog signaling. *Dev Biol* **319**, 132–145.

Case AP, Mitchell LE (2011) Prevalence and patterns of choanal atresia and choanal stenosis among pregnancies in Texas, 1999–2004. *Am J Med Genet A* **155A**, 786–791.

Clouthier DE, Hosoda K, Richardson JA, et al. (1998) Cranial and cardiac neural crest defects in endothelin-A receptor-deficient mice. *Development* **125**, 813–824.

Cobourne MT, Xavier GM, Depew M, et al. (2009) Sonic hedgehog signalling inhibits palatogenesis and arrests tooth development in a mouse model of the nevoid basal cell carcinoma syndrome. *Dev Biol* **331**, 38–49.

Cox TC (2004) Taking it to the max: the genetic and developmental mechanisms coordinating midfacial morphogenesis and dysmorphology. *Clin Genet* **65**, 163–176.

Diewert VM, Wang KY (1992) Recent advances in primary palate and midface morphogenesis research. *Crit Rev Oral Biol Med* **4**, 111–130.

Dufaure JP, Hubert J (1961) Table de developpement du lezard vivipare – Lacerta (Zootoca) vivipara jacquin. *Arch D Anat Microsc Morphol Exp* **50**, 309–328.

Dupe V, Matt N, Garnier JM, et al. (2003) A newborn lethal defect due to inactivation of retinaldehyde dehydrogenase type 3 is prevented by maternal retinoic acid treatment. *Proc Natl Acad Sci U S A* **100**, 14036–14041.

Eames BF, Schneider RA (2008) The genesis of cartilage size and shape during development and evolution. *Development* **135**, 3947–3958.

Ferguson MW (1981) The structure and development of the palate in *Alligator mississippiensis*. *Arch Oral Biol* **26**, 427–443.

Ferguson MW (1985) The reproductive biology and embryology of crocodilians. In *Biology of the Reptilia*. (eds Gans C, Billet F, Maderson PFA). New York: John Wiley and Sons.

Firnberg N, Neubuser A (2002) FGF signaling regulates expression of Tbx2, Erm, Pea3, and Pax3 in the early nasal region. *Dev Biol* **247**, 237–250.

Fish JL, Sklar RS, Woronowicz KC, et al. (2014) Multiple developmental mechanisms regulate species-specific jaw size. *Development* **141**, 674–684.

Fuchs A, Inthal A, Herrmann D, et al. (2010) Regulation of Tbx22 during facial and palatal development. *Dev Dyn* **239**, 2860–2874.

Gaare JD, Langman J (1980) Fusion of nasal swellings in the mouse embryo. DNA synthesis and histological features. *Anat Embryol (Berl)* **159**, 85–99.

Gong SG, Guo C (2003) Bmp4 gene is expressed at the putative site of fusion in the midfacial region. *Differentiation* **71**, 228–236.

Griffin JN, Compagnucci C, Hu D, et al. (2013) Fgf8 dosage determines midfacial integration and polarity within the nasal and optic capsules. *Dev Biol* **374**, 185–197.

Gui T, Osumi-Yamashita N, Eto K (1993) Proliferation of nasal epithelial and mesenchymal cells during primary palate formation. *J Craniofac Genet Dev Biol* **13**, 250–258.

Hall J, Jheon AH, Ealba EL, et al. (2014) Evolution of a developmental mechanism: species-specific regulation of the cell cycle and the timing of events during craniofacial osteogenesis. *Dev Biol* **385**, 380–395.

Hamburger V, Hamilton HL (1951) A series of normal stages in the development of the chick embryo. *J Morphol* **88**, 49–92.

He F, Xiong W, Yu X, et al. (2008) Wnt5a regulates directional cell migration and cell proliferation via Ror2-mediated noncanonical pathway in mammalian palate development. *Development* **135**, 3871–3879.

He F, Xiong W, Wang Y, et al. (2011) Epithelial Wntβ-catenin signaling regulates palatal shelf fusion through regulation of *Tgfβ3* expression. *Dev Biol* **350**, 511–519.

Higashihori N, Buchtova M, Richman JM (2010) The function and regulation of TBX22 in avian frontonasal morphogenesis. *Dev Dyn* **239**, 458–473.

Hsu P, Ma A, Wilson M, et al. (2014) CHARGE syndrome: a review. *J Paediatr Child Health* **50**, 504–511.

Hu D, Helms JA (1999) The role of sonic hedgehog in normal and abnormal craniofacial morphogenesis. *Development* **126**, 4873–4884.

Hu D, Marcucio RS (2009) A SHH-responsive signaling center in the forebrain regulates craniofacial morphogenesis via the facial ectoderm. *Development* **136**, 107–116.

Iamaroon A, Tait B, Diewert VM (1996) Cell proliferation and expression of EGF, TGF-α, and EGF receptor in the developing primary palate. *J Dent Res* **75**, 1534–1539.

Jankowski R (2011) Revisiting human nose anatomy: phylogenic and ontogenic perspectives. *Laryngoscope* **121**, 2461–2467.

Jiang R, Bush JO, Lidral AC (2006) Development of the upper lip: morphogenetic and molecular mechanisms. *Dev Dyn* **235**, 1152–1166.

Jin YR, Han XH, Taketo MM, et al. (2012) Wnt9b-dependent FGF signaling is crucial for outgrowth of the nasal and maxillary processes during upper jaw and lip development. *Development* **139**, 1821–1830.

Kim CH, Park HW, Kim K, et al. (2004) Early development of the nose in human embryos: a stereomicroscopic and histologic analysis. *Laryngoscope* **114**, 1791–1800.

Kosaka K, Hama K, Eto K (1985) Light and electron microscopy study of fusion of facial prominences. A distinctive type of superficial cells at the contact sites. *Anat Embryol (Berl)* **173**, 187–201.

Kurihara Y, Kurihara H, Suzuki H, et al. (1994) Elevated blood pressure and craniofacial abnormalities in mice deficient in endothelin-1. *Nature* **368**, 703–710.

Le Douarin NM, Brito JM, Creuzet S (2007) Role of the neural crest in face and brain development. *Brain Res Rev* **55**, 237–247.

Lee SH, Bedard O, Buchtova M, et al. (2004) A new origin for the maxillary jaw. *Dev Biol* **276**, 207–224.

MacDonald ME, Abbott UK, Richman JM (2004) Upper beak truncation in chicken embryos with the cleft primary palate mutation is due to an epithelial defect in the frontonasal mass. *Dev Dyn* **230**, 335–349.

Manzanares M, Nieto MA (2003) A celebration of the new head and an evaluation of the new mouth. *Neuron* **37**, 895–898.
McGonnell IM, Clarke JD, Tickle C (1998) Fate map of the developing chick face: analysis of expansion of facial primordia and establishment of the primary palate. *Dev Dyn* **212**, 102–118.
Minkoff R, Kuntz AJ (1977) Cell proliferation during morphogenetic change; analysis of frontonasal morphogenesis in the chick embryo employing DNA labeling indices. *J Embryol Exp Morphol* **40**, 101–113.
Oisi Y, Ota KG, Kuraku S, et al. (2013) Craniofacial development of hagfishes and the evolution of vertebrates. *Nature* **493**, 175–180.
Panchen AL (1967) The nostrils of choanate fishes and early tetrapods. *Biol Rev Camb Philos Soc* **42**, 374–420.
Parsons TS (1959) Nasal anatomy and the phylogeny of reptiles. *Evolution* **13**, 175–187.
Parsons TS (1968) Variation in the choanal structure of Recent turtles. *Can J Zool* **46**, 1235–1263.
Parsons TS (1971) *Anatomy of Nasal Structures from a Comparative Viewpoint*, Berlin: Springer.
Patterson SB, Johnston MC, Minkoff R (1984) An implant labeling technique employing sable hair probes as carriers for 3H-thymidine: applications to the study of facial morphogenesis. *Anat Rec* **210**, 525–536.
Peterka M, Sire JY, Hovorakova M, et al. (2010) Prenatal development of *Crocodilus niloticus niloticus* Laurenti, 1768. *J Exp Zool B Mol Dev Evol* **314**, 353–368.
Reid BS, Yang H, Melvin VS, et al. (2011) Ectodermal Wnt/β-catenin signaling shapes the mouse face. *Dev Biol* **349**, 261–269.
Richman JM (1992) The role of retinoids in normal and abnormal embryonic craniofacial morphogenesis. *Crit Rev Oral Biol Med* **4**, 93–109.
Richman JM, Lee SH (2003) About face: signals and genes controlling jaw patterning and identity in vertebrates. *BioEssays* **25**, 554–568.
Richman JM, Tickle C (1989) Epithelia are interchangeable between facial primordia of chick embryos and morphogenesis is controlled by the mesenchyme. *Dev Biol* **136**, 201–210.
Richman JM, Herbert M, Matovinovic E, et al. (1997) Effect of fibroblast growth factors on outgrowth of facial mesenchyme. *Dev Biol* **189**, 135–147.
Ruest LB, Xiang X, Lim KC, et al. (2004) Endothelin-A receptor-dependent and -independent signaling pathways in establishing mandibular identity. *Development* **131**, 4413–4423.
Sato T, Kurihara Y, Asai R, et al. (2008) An endothelin-1 switch specifies maxillomandibular identity. *Proc Natl Acad Sci U S A* **105**, 18806–18811.
Schweitzer DN, Graham JM Jr, Lachman RS, et al. (2001) Subtle radiographic findings of achondroplasia in patients with Crouzon syndrome with acanthosis nigricans due to an Ala391Glu substitution in FGFR3. *Am J Med Genet* **98**, 75–91.
Som PM, Naidich TP (2013) Illustrated review of the embryology and development of the facial region, part 1: early face and lateral nasal cavities. *AJNR Am J Neuroradiol* **34**, 2233–2240.
Som PM, Naidich TP (2014) Illustrated review of the embryology and development of the facial region, part 2: late development of the fetal face and changes in the face from the newborn to adulthood. *AJNR Am J Neuroradiol* **35**, 10–18.
Song Y, Hui JN, Fu KK, et al. (2004) Control of retinoic acid synthesis and FGF expression in the nasal pit is required to pattern the craniofacial skeleton. *Dev Biol* **276**, 313–329.
Song L, Li Y, Wang K, et al. (2009) Lrp6-mediated canonical Wnt signaling is required for lip formation and fusion. *Development* **136**, 3161–3171.
Swibel Rosenthal LH, Caballero N, Drake AF (2012) Otolaryngologic manifestations of craniofacial syndromes. *Otolaryngol Clin North Am*, **45**, 557–577, vii.
Szabo-Rogers HL, Geetha-Loganathan P, Nimmagadda S, et al. (2008) FGF signals from the nasal pit are necessary for normal facial morphogenesis. *Dev Biol* **318**, 289–302.
Szabo-Rogers HL, Smithers LE, Yakob W, et al. (2010) New directions in craniofacial morphogenesis. *Dev Biol* **341**, 84–94.
Tamarin A, Crawley A, Lee J, et al. (1984) Analysis of upper beak defects in chicken embryos following with retinoic acid. *J Embryol Exp Morphol* **84**, 105–123.
Trasler DG (1968) Pathogenesis of cleft lip and its relation to embryonic face shape in A-J and C57BL mice. *Teratology* **1**, 33–49.
Warbrick JG (1960) The early development of the nasal cavity and upper lip in the human embryo. *J Anat* **94**, 351–362.
Wedden SE (1987) Epithelial-mesenchymal interactions in the development of chick facial primordia and the target of retinoid action. *Development* **99**, 341–351.
Werneburg I, Hugi J, Muller J, et al. (2009) Embryogenesis and ossification of *Emydura subglobosa* (Testudines, Pleurodira, Chelidae) and patterns of turtle development. *Dev Dyn* **238**, 2770–2786.
Will LA, Meller SM (1981) Primary palatal development in the chick. *J Morphol* **169**, 185–190.
Yee GW, Abbott UK (1978) Facial development in normal and mutant chick embryos. I. Scanning electron microscopy of primary palate formation. *J Exp Zool* **206**, 307–321.
Young NM, Hu D, Lainoff AJ, et al. (2014) Embryonic bauplans and the developmental origins of facial diversity and constraint. *Development* **141**, 1059–1063.

Supporting Information

Additional Supporting Information may be found in the online version of this article:

Video S1. Fly-through frontal sections of 15 dpo crocodile (*Crocodilus niloticus*) through the region of the nasal cavities.
Video S2. Rotational movie of a stage 27 chicken embryo nasal cavity prior to fusion.
Video S3. Rotational movie of a stage 28 chicken embryo just after initial fusion has occurred between the frontonasal mass and anterior maxillary prominence.
Fig. S1. Schematic depicting the processes of fusion and merging in the primary palate.
Fig. S2. Crocodilian choana formation.
Fig. S3. High power views of the choanae in chicken, non-avian reptiles and mammals.
Fig. S4. BrdU labeling of a stage 31 bearded dragon (*Pogona vitticeps*) visible in coronal section at similar level as in chicken in Figure 5.
Fig. S5. Schematic summarizing the conserved steps and branching points during choana formation.
Table S1. Statistical analysis using analysis of variance (ANOVA) followed by Fisher's LSD post-hoc testing on percent labeled cells/total cell number on chicken choanal regions presented in Fig. 5D.